

Electronic Supporting Information

Photoelectrochemical Hydrogen Generation employing a Cu_2O -based Photocathode with improved Stability and Activity by using Ni_xP_y as the cocatalyst.

Manjeet Chhetri and C. N. R. Rao*

Materials and Chemicals: Copper sulfate pentahydrate [Sigma Aldrich, $\text{CuSO}_4 \cdot 5\text{H}_2\text{O}$], Lactic acid [SD Fine Chem. India], Sodium Hydroxide [Sigma Aldrich, NaOH], FTO slide [Sigma Aldrich, surface resistivity $\sim 7 \text{ ohm/cm}^2$], Nickel Acetate [Sigma Aldrich, $\text{Ni}(\text{OAc})_2$], Phosphoric acid [H_3PO_4 SD Fine Chem. India], Phosphorous acid [H_3PO_3 SD Fine Chem. India], N-methylformamide (NMF) [SD Fine Chem. India], Cu wires, Enamel remover, Ag paste.

Characterizations: Powder X-ray diffraction (PXRD) of photoanodes was recorded using a Bruker AXS D8 Discover diffractometer attached with Cu $\text{K}\alpha$ radiation. X-ray photoelectron spectroscopy (XPS, Mg- $\text{K}\alpha$ X ray source, 1253.6 eV) was recorded to analyze the surface composition of samples. UV-Vis absorption spectra were examined using a UV-Perkin Elmer UV/Vis spectrometer. Transmission electron microscopy (TEM, Technai F30 UHR, 200 kV) was used to study the crystal morphology and composition (HRTEM) and Field emission scanning electron microscopy (FESEM, FEI Quanta operated at 15 kV, equipped with EDAX) was used to investigate the composition, morphology and thickness of various layers in electrodes. The elemental ratios of the as prepared electrodes were confirmed by optical emission spectrometry-inductively coupled plasma spectrometry (OES-ICP) (Perkin Elmer Optima 7000 DV).

Sample Preparation for Characterizations: For XPS analysis the deposited electrode as kept in ambient atmosphere were directly used without any further processing. Mg- $\text{K}\alpha$ X ray was used as non-monochromatic source with hemispherical electron energy analyzer.

Electrochemical Impedance Spectroscopy analysis: The data points were fitted by CHI760E inbuilt software (Model 700E Series Electrochemical Analyzer/Workstation, CHI Inc., with simulations and fitting commands) by proposing an equivalent modified Randles' circuit model described. An impedance simulator is integrated into the program. The fitting error is ~ 0.01 and elapsed time ~ 450 seconds. The symbols represent the experimental data and the lines represents fitting results utilizing the equivalent circuit.

Circuit Element Properties: R=Resistor; C=Capacitor; Q= Constant phase element; j=current density; ω = frequency

Element	Impedance	Conductance	Phase
R (resistor)	$Z_R = R$	$Y_R = 1/R$	$\Phi = 0$
C (capacitor)	$Z_C = -j/C$	$Y_C = j\omega C$	$\Phi = \pi/2$
Q (phase)	$Z_Q = (j\omega)^{-n}/Y_0$	$Y_Q = (j\omega)^n Y_0$	$\Phi = n\pi/2, 0 < n < 1$

Reference- CHI Instruments Manual; J. R. Macdonald, *Ann. Biomed. Eng.*, 20, 289-305 (1992) or "Impedance Spectroscopy", E. Barsoukov and J. R. Macdonald, Wiley, Hoboken, 1987 (1st ed), 2005 (2nd ed).

X-Ray Photoelectron Spectroscopy analysis: XPS analysis was done using XPSPEAK4.1 software. Background subtraction was performed using Shirley functions with the optimizations to bring the Shirley background data points which are higher than the signal intensities at some points. The optimization helps in increasing the slope value until the Shirley background is below the signal intensities. To add peaks for the deconvolution of XPS core level peak, Gaussian-Lorentzian sum function was used with adjustable parameters like peak position, peak area, FWHM and % Gaussian-Lorentzian functions. Depending on the number of anticipated peaks, the peak were deconvoluted by adjusting the parameters until the final combined peak from various added peaks matched with the actual data obtained from XPS measurement (raw data).

XPS Discussion: In the X-Ray photoelectron spectroscopy (XPS) distinction between the Cu_2O and CuO phases could be made from the binding energies of the $\text{Cu } 2p_{1/2}$ and $2p_{3/2}$. Core level XPS spectra of photocathode thin films are plotted in **Fig. 1b** with respective peak positions of the $\text{Cu } 2p_{1/2}$ and $2p_{3/2}$ along with satellite peaks. The $\text{Cu } 2p$ ($1/2$ and $3/2$) peaks at 952.7 and 933 eV could be deconvoluted to Cu^{2+} and Cu^+ individual peaks which also gives the relative proportion of Cu_2O and CuO close to that obtained from the $\text{O } 1s$ peak deconvolution. Ni_{12}P_5 and some Ni_5P_4 constituted Ni_xP_y .

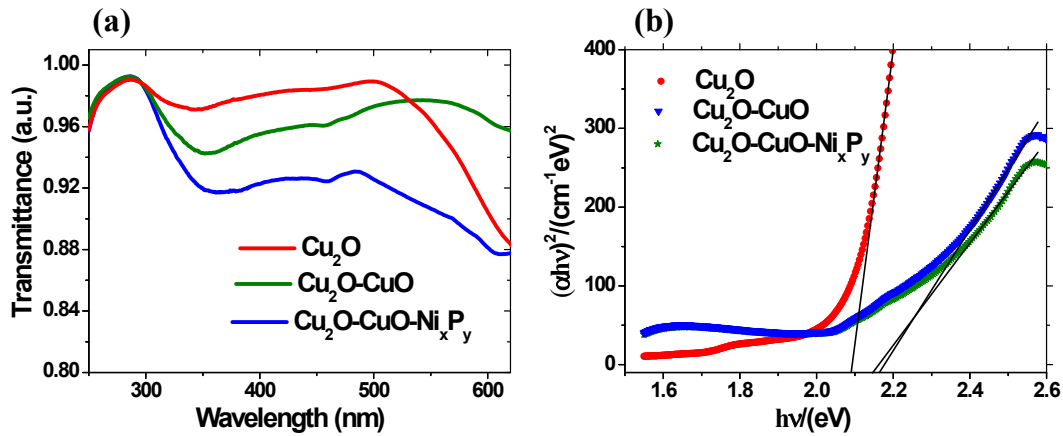


Fig. S1: (a) Optical absorption (UV-NIR) spectra spectrum of the bare Cu_2O (red) and the Heterostructures of $\text{Cu}_2\text{O-CuO}$ (green) and $\text{Cu}_2\text{O-CuO-Ni}_x\text{P}_y$ (blue) thin films deposited on FTO. (b) The Tauc plot and band gap determination of the thin film electrodes. Colours have their defined representations.

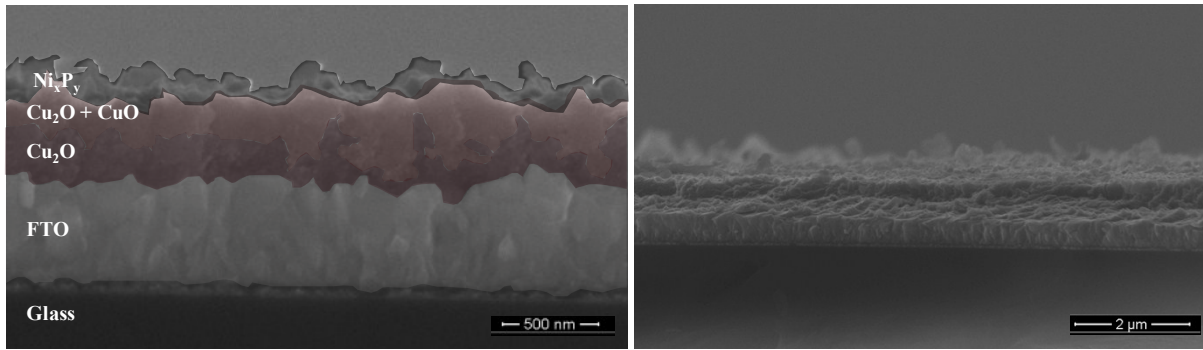


Fig. S2: Cross Sectional FESEM images of $\text{Cu}_2\text{O-CuO-Ni}_x\text{P}_y$ showing the representative gradual layers of hetero-interfaces (approximation in the thickness of different layers).

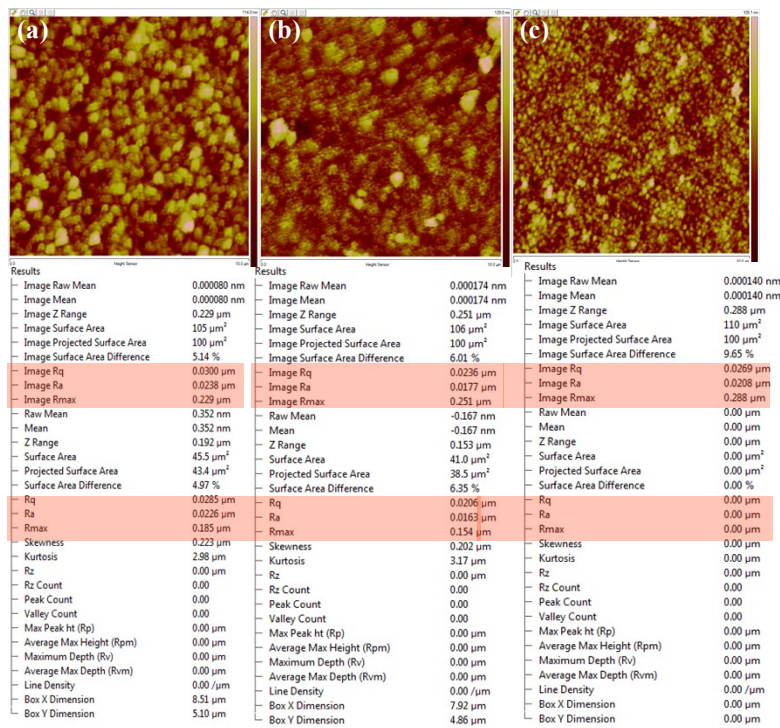


Fig. S3: Detailed AFM topographic analysis of the electrode surfaces for estimation of roughness factor and grain size study (a) Cu_2O (b) $\text{Cu}_2\text{O-CuO}$ and (c) $\text{Cu}_2\text{O-CuO-Ni}_x\text{P}_y$.

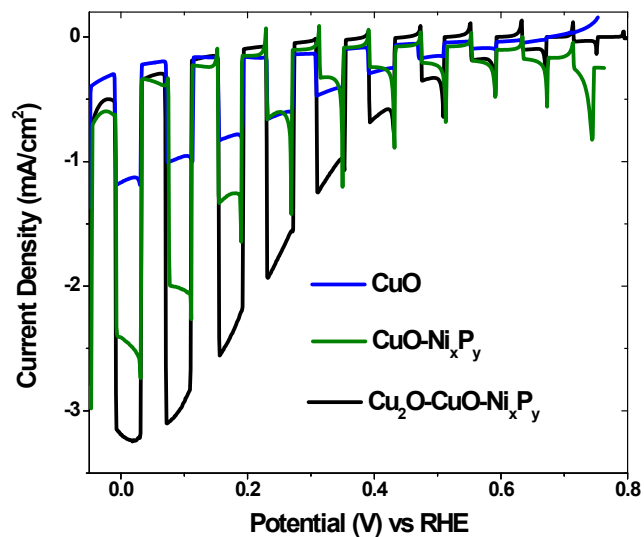


Fig. S4: Current–Voltage (I-V) characteristics of a photocathodes: PEC hydrogen evolution activity comparison with and without the Cu₂O-CuO interface to understand the efficiency of photocathode and the role of CuO. All measurements were carried out in pH-7, 0.5 M Na₂SO₄ electrolyte under chopped light irradiation.

Stability of catalyst after PEC study:

The FESEM images before and after 1 hour PEC activity (amperometric I-t study at 0.05 V vs RHE) suggests that after the PEC study morphology changes with more particles on surface causing the smooth electrode surface to be rough although resulting in very slight decrease in photocurrent efficiency.

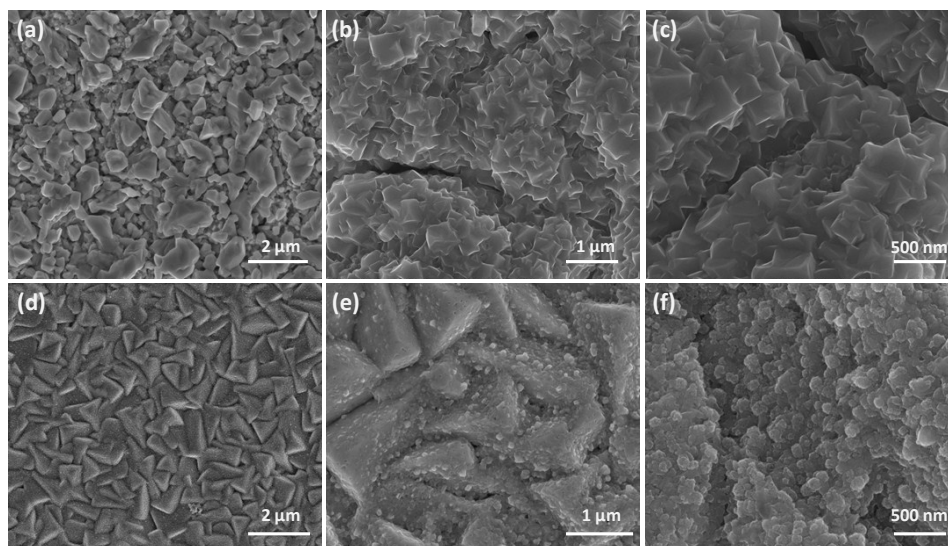


Fig. S5: Morphology study of electrode: FESEM images of the electrode (a-c) before PEC study and (d-f) after PEC study.

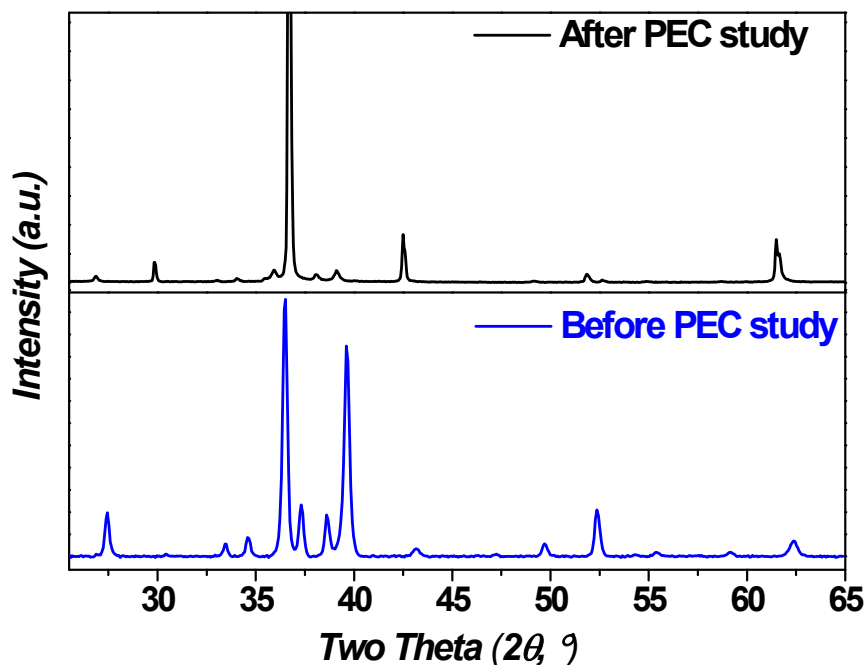


Fig. S6: X-ray diffraction patterns of $\text{Cu}_2\text{O-CuO-Ni}_x\text{P}_y$ before and after PEC study (1 hour chronoamperometric i-t study at 0.05 V vs RHE) to study the stability of the photoelectrode.

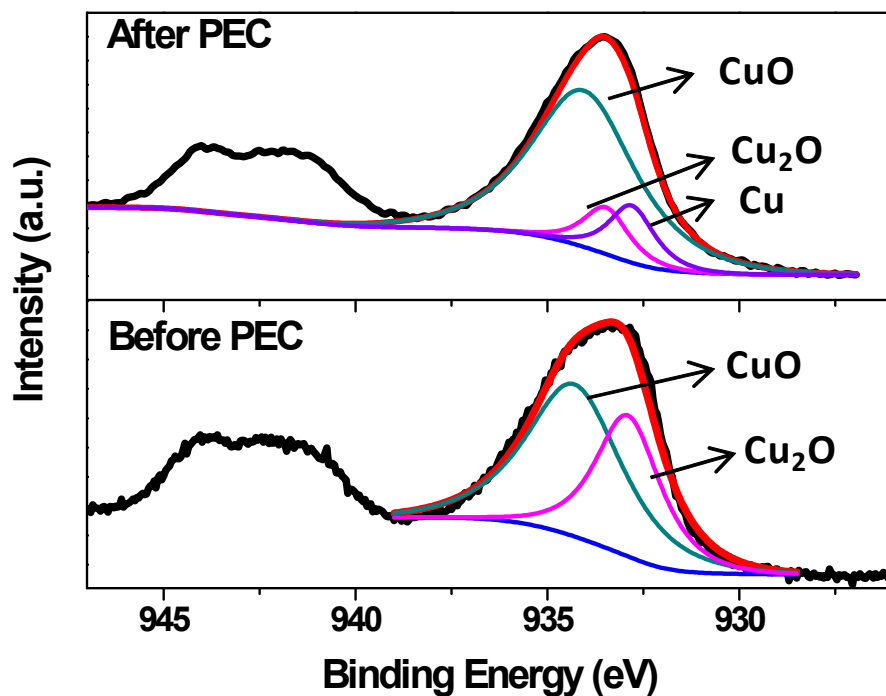


Fig S7: Core level X-ray photoelectron spectra for Cu-2p_{3/2} on the surface of the $\text{Cu}_2\text{O-CuO-Ni}_x\text{P}_y$ electrode before and after PEC stability test. The shaded portion represents the shake of satellite peaks which is more prominent in after PEC sample suggesting greater fraction of CuO on the electrode surface resulting from the photocorrosion.

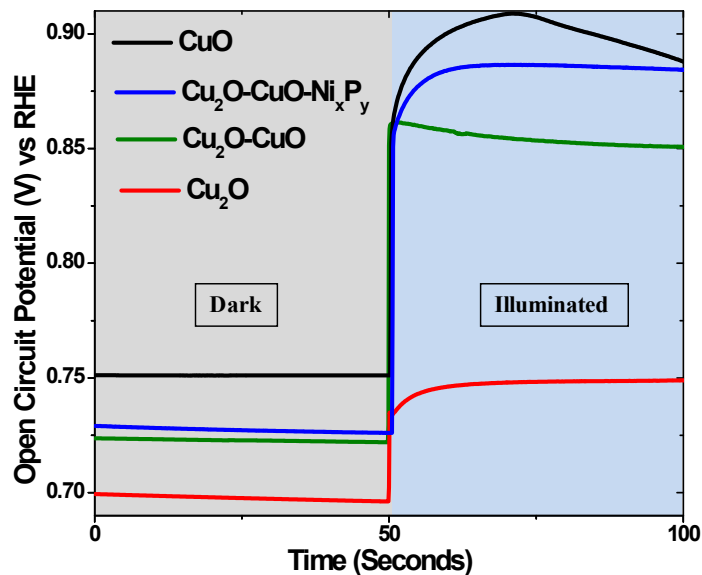


Fig.S8: Open circuit potential vs time graph of the photocathodes in dark and illuminated conditions obtained by chopping of incident light.

PEC H₂ evolution activity of Cu₂O-CuO-NiO: study of PEC activity with other cocatalyst

Cu₂O-CuO-NiO electrode was fabricated by the method used for other electrodes in this study except in the last step. Pulse plating electrodeposition of Ni(OH)₂ was carried out from a solution of 0.5 M Nickel acetate in 5wt% NMF (without the phosphorous source). The electrodeposition parameters were the same. After deposition the film annealed at 400°C for 30 mins (5°C/min heating rate). The photocurrent study for hydrogen evolution with NiO as cocatalyst suggests that Ni_xP_y is better for HER. This is obvious because of the superior electrochemical HER activity of Ni_xP_y than that of NiO.

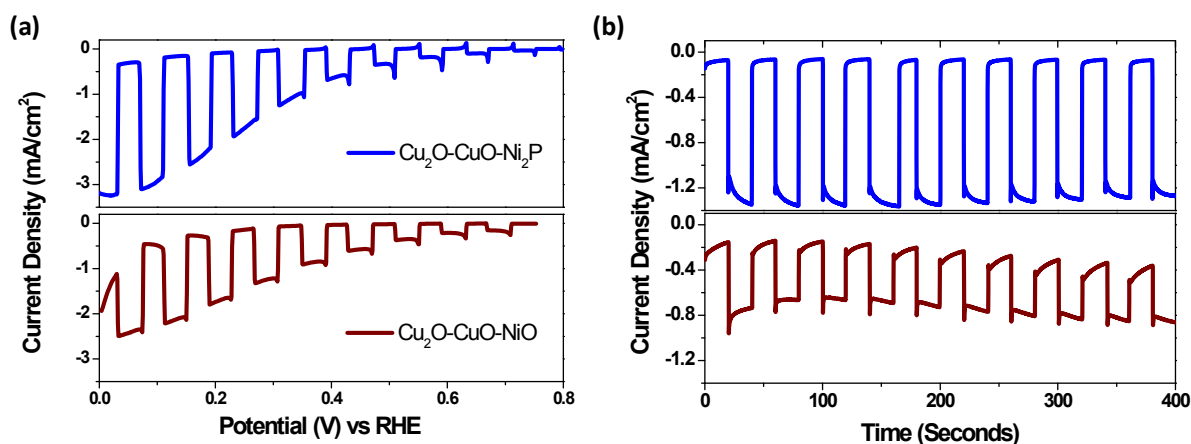


Fig. S9: Comparison of PEC activity with NiO as cocatalyst: (a) LSV curve at same conditions as when Ni_xP_y is used as cocatalyst. (b) Transient photocurrent stability test for both the catalysts with Ni_xP_y and NiO as cocatalyst.